

A solid-state growth of Ag nanowires and analysis of self-growing process on a bio-polymer chitosan film

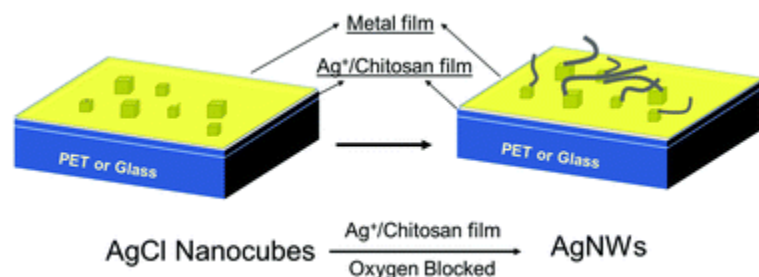
By: Harish Chevva, Rakkiyappan Chandran, [Dennis LaJeunesse](#), and [Jianjun Wei](#)

H. Chevva, R. Chandran, D. LaJeunesse, J. Wei, A solid-state growth of Ag nanowires and analysis of self-growing process on a bio-polymer chitosan film, *New Journal of Chemistry*, 2019, 43, 3529-3535. <https://doi.org/10.1039/C8NJ05729J>

***© 2019 The Royal Society of Chemistry and the Centre National de la Recherche Scientifique. Reprinted with permission. No further reproduction is authorized without written permission from the Royal Society of Chemistry. This version of the document is not the version of record. ***

Abstract:

The growth mechanism of silver nanowires (AgNWs) in solution has been thoroughly investigated and it has been demonstrated that factors like oxidative etching and inclusion of Cl^- ions in the reaction system play critical roles in the formation of AgNWs. This research is the first to report the growth mechanism of AgNWs in the solid state on a chitosan polymer film with respect to factors such as oxidative etching, Cl^- ions and time. The AgNW synthetic method is a green process that involves aqueous solvents for film preparation and ambient conditions for AgNW growth. It is demonstrated that the source of the silver precursor for this solid state AgNW growth is the cuboidal AgCl nanoparticles that form during the solution preparation. Furthermore, it is shown that the $\langle 111 \rangle$ crystal faces of these cuboidal AgCl nanoparticles are the nucleation sites of AgNW growth. Unlike solution-based AgNW synthetic processes, the AgNWs generated by the chitosan film-based method are irregular and present lateral as well as longitudinal growth, which suggests a slightly different mechanism from the solution-based AgNW growth.



Keywords: oxidative etching | silver nanowires | nanostructures | chloride ions

Article:

Introduction

The methods for synthesizing one dimensional (1D) nanostructures are divided into two strategies: bottom-up methods and top-down methods.^{1,2} The growth mechanisms of

nanowires *via* various synthetic methods have been studied.³⁻⁶ In all bottom-up methods, the fabrication of the material is controlled at the atomic level and involves the ordering of atoms during the formation of 1D nanostructures such as nanowires. Bottom-up solution synthesis methods of 1D nanomaterials⁷ include templated growth with 1D morphologies to direct the formation of 1D nanostructures,⁸ super saturation control to modify the growth habit of a seed,⁹ capping agents to kinetically control the growth rates of various facets of a seed,¹⁰ and self-assembly of 0D nanostructures into 1D nanostructures.^{11,12} Bottom-up approaches, both solution and solid-state processes, have been used to generate a wide variety of 1D nanomaterials but only a few approaches have been used to generate metallic 1D nanomaterials and none of these methods involves a solid-state approach in polymer films. The chitosan thin film-based AgNW synthetic process that we have reported,^{13,14} to the best of our knowledge, is the first solid-state bottom-up fabrication method for the synthesis of 1D metal nanostructures in biopolymer thin films.

Currently the available methods to synthesize solid state semiconducting nanowires¹⁵⁻¹⁷ and metal nanowires¹⁸⁻²⁰ involve a top-down approach in which 1D nanostructures are fabricated using advanced laboratory lithographic techniques like E-Beam, Focus Ion Beam (FIB), UV lithography and Reactive Ion Etching (RIE). This method of fabrication is expensive, labor intensive, and economically unfeasible for scale up when compared to current bottom-up approaches.^{2,21} Most solution-based silver nanoparticle or nanowire synthetic methods involve the use of polyvinylpyrrolidone (PVP) as a reducing and stabilizing agent, requiring high temperature, *e.g.* 180 °C.^{22,23} Some improvement has been made in terms of shortened reaction time, crystal control and temperature.²⁴⁻²⁶ Recently, there have been several methods of silver nanoparticle synthesis which use the chitosan polymer or biomaterials as a stabilizing/reducing agent.²⁷⁻³¹ Among these reports, our published work demonstrates a facile green method to synthesize Ag NPs on chitosan film, which eventually grow in the solid-state synthesis of AgNWs.^{13,14} In previously described AgNW synthetic processes, the growth mechanism for AgNWs in solution relies on several influencing factors including oxidative etching,^{32,33} concentration of Cl⁻ ions,³⁴ thermodynamics, specifically the temperature at which the synthesis reaction is performed,^{35,36} and the kinetics of the reaction system, specifically the time and intensity of mechanical agitation.¹⁰

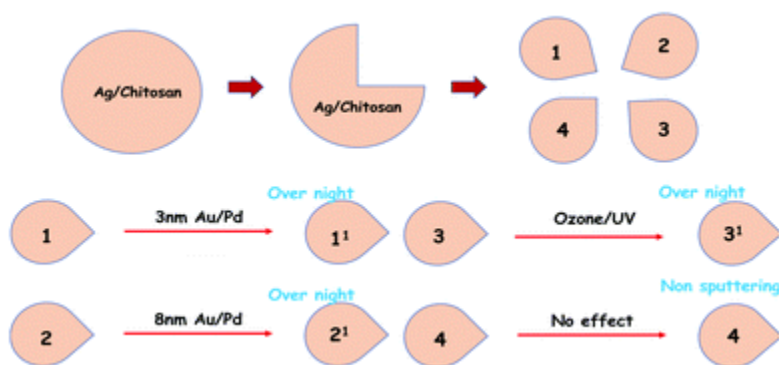
Herein we report the growth mechanism of AgNWs *via* a bottom up synthetic method for the generation of AgNWs on a chitosan bio-polymer film. This method is distinct from other established methods of AgNW synthesis, as it is a solid-state process that is performed under mild conditions. In this article, the conditions that control the AgNW growth on the chitosan thin film in the solid state synthesis process have been tested. The growth of the AgNWs in a solid-state medium is observed and described. We have found that the key factors (*e.g.* oxidation, Cl⁻ ion, and time) that influence the synthesis of AgNWs in solution play different roles in the chitosan solid-state AgNW growth.

Results and discussion

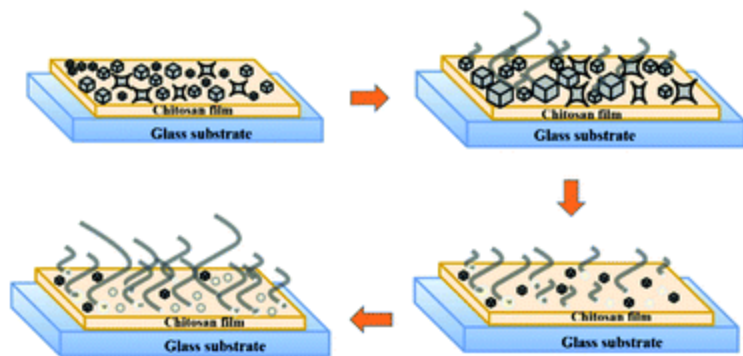
Oxidative etching

Oxidative etching has been demonstrated to inhibit the growth of AgNWs in solution-based AgNW synthesis.³⁷ This inhibition has been described mechanistically to be due to the oxidative etching, *i.e.* the attack of oxygen atoms to multiply twinned seeds. The thermodynamically stable multiply twinned seeds are the source for AgNW growth in many solution-based processes. Single crystal seeds that are the source for the formation of Ag NPs are more resistant to oxidative etching since they lack twin boundary defects on their surface. With the intrusion of oxygen atoms into the reaction solution, the oxygen atoms attach to twinned crystals and dissociate them back to single crystal seeds as described in a previous article, hindering the possibility of the growth of AgNWs in the solution.³²

In solution AgNW synthetic processes, there are three steps which illustrate the role of oxidation as an inhibitor of AgNW growth:³⁷ (1) removal of O₂ interference in the reaction system by performing the reaction in an inert gas environment; (2) use of capping agents like citrate to prevent oxygen from being adsorbed to the seeds; and (3) the presence of redox pairs, such as Fe^{III/II} and Cu^{II/I} salts, which scavenge oxygen in the reaction solution.³⁴ In chitosan AgNW solid state synthesis, we tested whether oxygen removal is essential for the growth of AgNWs. In this manuscript, we demonstrate a new method of reducing oxidation in the polymer-based AgNW reaction system which we call smothering. In previous reports of the chitosan film synthesis of AgNWs,^{13,14} the films of chitosan that contained silver nanoparticles were sputter coated on a thin Au/Pd film. The metal-coated chitosan film resulted in the AgNW growth, while those left uncovered did not. To determine whether a nanometer thick layer of Au/Pd was sufficient to prevent exposure to oxygen and to determine whether the presence of oxygen was inhibitory to the solid state AgNW growth, we performed the following experiment (Scheme 1). A single thin film of chitosan containing silver nanoparticles was prepared as described earlier¹³ and divided into four pieces: quadrant '1' was coated with 3 nm of Au/Pd, quadrant '2' was coated with 8 nm of Au/Pd, quadrant '3' was treated with oxygen plasma to promote oxidation, and quadrant '4' was unprocessed. All the treated film quadrants are denoted as '1¹', '2¹' and '3¹', respectively as shown in Scheme 2 below. The samples were then stored in dry air and examined after one day and then a week after for the growth of Ag NWs.



Scheme 1. Schematic illustration of the proposed experiment to prove that Au/Pd coating of the Ag NPs/chitosan film yields AgNW growth.



Scheme 2. Schematic depiction of the solid state bottom-up AgNW growth pathway.

Since our hypothesis is that oxygen will inhibit AgNW growth in the solid state, it is expected that the thin films that are uncoated ('4') or plasma etched with an oxygen etch ('3¹') should have little or no AgNWs after a week of growth, while the thin films coated with varying amounts of Au/Pd metal ('1¹ & 2¹') will have AgNWs. To verify this, SEM was performed to characterize the films as shown in Fig. 1.

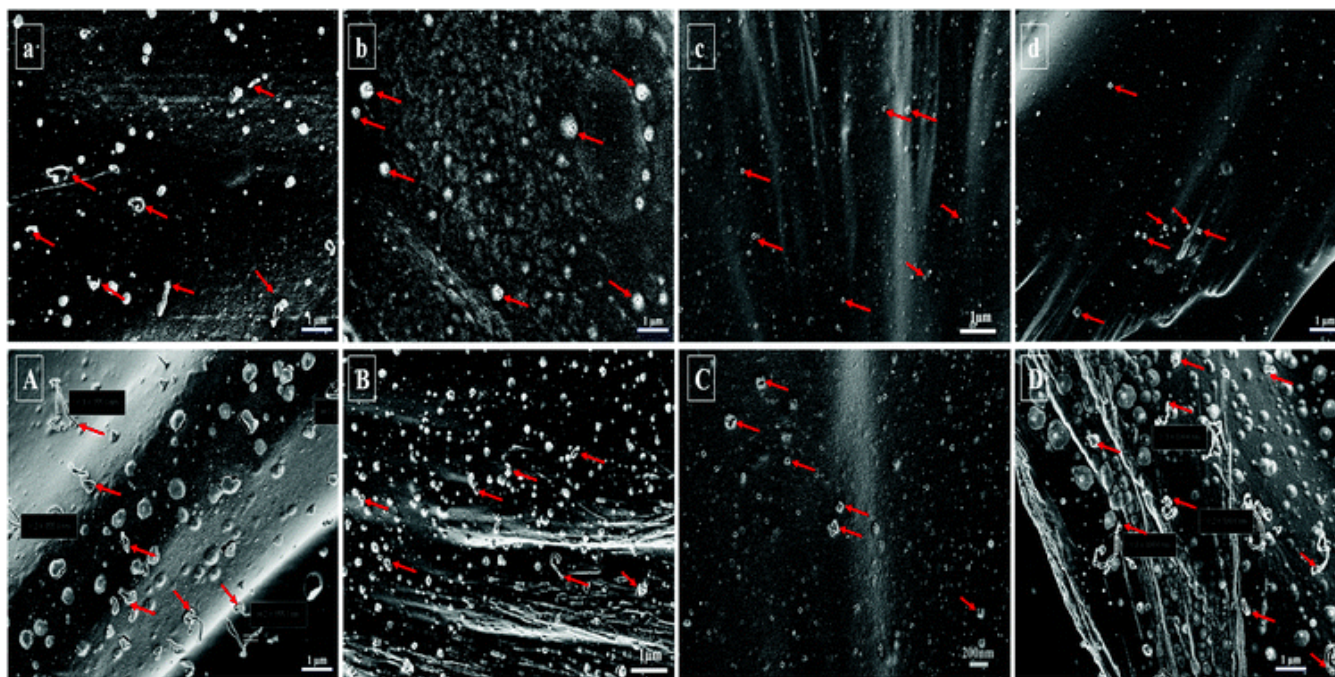


Fig. 1 (a, b, c and d) SEM images of the films 1, 2, 3 and 4 respectively stored overnight. (A, B, C and D) SEM images of Ag films 1¹, 2¹, 3¹ and 4 respectively stored for one week.

As expected, we observed the growth of AgNWs on the film with a 3 nm coating of Au/Pd and stored overnight at room temperature (Fig. 1a, with pointed arrows indicating growth initiation of AgNWs). The one-day old AgNWs are small with an average diameter of 90 ± 10 nm and an average length of 500 ± 50 nm. For the films with an 8 nm coating of Au/Pd and stored the same way (Fig. 1b), AgNW growth initiation was also observed by small protrusions of Ag NWs on the film (Fig. 1b, arrows). It is noted that the thickness of the 8 nm Au/Pd coating obscures much of the details of the wire. However, there is no growth of AgNWs on the film treated with

oxygen plasma (Fig. 1c); in fact, we observed the breakage of the cubic particles on the film surface. For the untreated film in quadrant 4, we only observed the cubic particles within the chitosan film surface (Fig. 1d). This indicates that ambient oxygen can inhibit the AgNW growth on the film ('4').

In the samples stored for one week, we observed a similar trend of further increase in the size of the Ag NWs (Fig. 1A). The Ag NWs on the film with the 3 nm coating of Au/Pd had an average length of $3 \pm 1 \mu\text{m}$ and an average diameter of $150 \pm 10 \text{ nm}$. In the film with the 8 nm coating of Au/Pd, Ag NWs growing out of the film are clearly observed (Fig. 1B). One week old Ag NWs have an increased aspect ratio when compared to one day old Ag NWs, demonstrating that these wires grow laterally as well as longitudinally. This is distinct from solution-based AgNW growth processes where the AgNWs mainly grow longitudinally. The chitosan films that were exposed to oxygen plasma, even after a week's time, showed no trace of Ag NW growth (Fig. 1C). This proves the hypothesis regarding the effect of oxygen on the surface of the film in hindering the growth of Ag NWs. In the case of the quadrant '4' film, initially when it was exposed to oxygen in air for one day, no growth of Ag NWs (Fig. 1d) was observed. The same section '4' of the film was coated with Au/Pd to block oxygen exposure for SEM characterization after a week, and clear growth of Ag NWs was seen on the film (Fig. 1D) though shorter than samples 1 and 2. This proves that the growth initiation of Ag NWs can take place once isolated from oxygen even after a week of exposing the film to air.

We extended this study further by examining the smothering of the chitosan thin film with a PVD deposition of a 5 nm Au layer and (ESI† Fig. S1) and a self-assembled monolayer of 400 nm polystyrene beads (Fig. 2).³⁸ Similar to the sputter coated samples, the growth initiation of AgNWs from the corners of the cubic Ag nanoparticles was observed on the PVD Au coated chitosan thin films and later the AgNWs grew longer and thicker. For the 400 nm bead covered films, the AgNWs sprout out from the bottom of the beads by pushing the beads away (Fig. 2b). These experiments further prove that blocking oxidative etching is necessary for the solid state growth of Ag NWs.

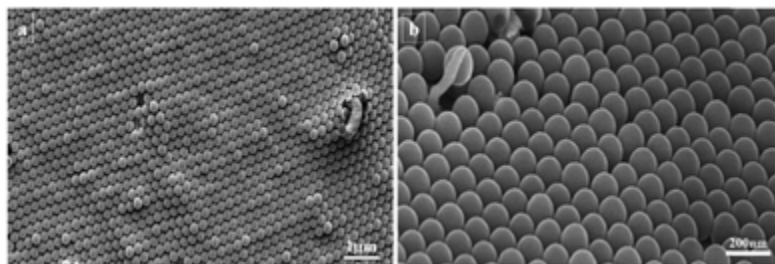


Fig. 2 SEM images of the Ag/chitosan film coated with self-assembled polymer beads of 400 nm size. With aging of the film the Ag NW growth pushing the polymer bead out is seen.

Role of Cl^- ions

Chloride ions have been demonstrated to play a critical role in the synthesis and growth of Ag NWs.³⁴ In polyol AgNW synthesis, PVP reacts with NaCl to generate free Cl^- ions which promote the formation of a silver chloride precipitate that serves as the source of Ag^+ ions for the growth of Ag NWs.³⁴ In our first synthesis process, 1 ml of 100 mM NaCl solution was added to

the chitosan solution with magnetic stirring. Furthermore, when a silver precursor AgNO_3 solution was added to the above solution, a white precipitate was formed as shown in Fig. 3a. This white precipitate of AgCl further vanished in the synthesis process to form pink plasmonic color of Ag solution as shown in Fig. 3a (right). The pink color solution was used to form films for the study of the solid-state growth of AgNWs .

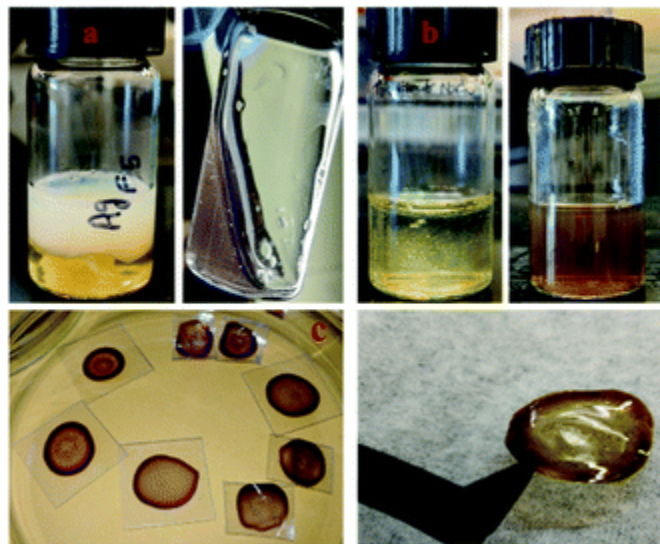


Fig. 3 Experimental images of synthesis of Ag NPs with NaCl in chitosan solution. (a) AgCl white precipitate formation. (b) After synthesis plasmonic color Ag NP solution. (c) Thin film formed from the Ag NP solution which serves as a base for Ag NW growth.

It has been hypothesized that residual silver chloride in the chitosan thin film serves as the source of silver needed for the growth of AgNWs . To test this hypothesis, the chitosan solution without addition of sodium chloride was prepared and used as a control as shown in Fig. 3b. It can be seen that there is no white precipitate formed and the solution shows a plasmonic green color (Fig. 3b, right). Films are made on PET with the solution by following the same procedure as that for AgNW synthesis on Ag /chitosan films (Fig. 1).

The NaCl added (Fig. 3a) or non-added (Fig. 3b) films are characterized using SEM, UV-Vis, XRD and EDS. SEM analysis of the chitosan/ Ag NP thin film formed without NaCl is shown in ESI† data Fig. S2, which demonstrates that the Ag NPs are spherical. UV-Vis spectral analysis (Fig. S3, ESI†) shows the difference between the non- NaCl generated chitosan/ Ag NP thin films and those with NaCl . The film generated without NaCl shows the presence of a sharp absorption peak at 420 nm which signifies the uniform distribution of small sized spherical Ag NPs in the film.³⁹ The XRD plot depicted in Fig. S3c (ESI†) shows sharp AgCl peaks at (111), (200), (311), (222) and (311) for the film with NaCl ,⁴⁰ suggesting the presence of residual AgCl in the formed films. At the same time, Ag peaks at (111), (200), (220), and (222) were obtained, indicating the Ag crystallization. For the film prepared without NaCl (Fig. S3d, ESI†), there is no sign of AgCl peaks in the XRD plot, but Ag peaks were observed.

To further understand the role of Cl^- ions, varying concentrations of NaCl from 1 mM to 100 mM were added respectively to the reaction process and films were made with the solution as explained previously. UV-Vis absorption peaks were observed both for the solution form and the

film form of the same (Fig. S4, ESI†). No obvious absorption was observed for the solution and the film prepared without NaCl. When NaCl was added, a plasmonic absorption peak at around 420 nm was observed, indicating the generation of Ag NPs and AgCl nanocubes.⁴¹ The absorption peak of plasmonic Ag was observed to be broadened and red shifted with the increase in the concentration of NaCl and in the presence of AgCl cubic structures.⁴¹ Both the solution and film data follow a similar trend.

These films were further characterized by XRD to observe the crystal structure of Ag and NaCl on the films with the increase in the concentration of NaCl. Note that Ag NWs were formed in the films. Fig. S5 (ESI†) shows the collation of XRD peaks of all the films ranging from no NaCl concentration to 100 mM concentration of NaCl. With the increase in the NaCl concentration, AgCl XRD peaks were observed. Meanwhile, the structural characteristics of the Ag NW XRD peaks were maintained. The (111) phase of the Ag NWs stayed dominant among the Ag crystal peaks.

EDS was used for elemental analysis (Fig. S6 and S7, ESI†). The results for the non-NaCl thin films (Fig. S6a and S7a, ESI†) showed that the spherical particles seen in Fig. S2 (ESI†) did not have any chlorine. The mean average value (MV) percentage of Na 0%, Cl 0% and Ag of 50% was obtained for the film made from Ag/chitosan solution without addition of NaCl. In contrast, the cubic nanoparticles in the chitosan/Ag NP thin film made with NaCl have chlorine (Fig. S6b–d, ESI†). Fig. S7b–d (ESI†) show the SEM imaging and EDS analysis of the Ag/chitosan film with addition of NaCl. Each figure shows the analysis at different storage times of the same film to allow the AgNWs to grow on the film. From the EDS analysis shown in Fig. S6b and S7b (ESI†), where the analysis was carried out using distributed cubic nanostructures on the film, the MV percentage of Na was 2.45%, Cl was 1.56% and Ag was 18.96%. With the MV of Cl and Ag observed on the cubic structures, the composite of the cubic nanostructures can be confirmed as AgCl. With further storage time of the film with the growth of Ag NWs, the EDS analysis of the film showed MV percentages of Na as 1.46%, of Cl as 0.65% and of Ag as 35.62%. The increase in the percent mass of Ag and decrease in the percentage mass of Cl support the idea that the cubic AgCl nanoparticles served as the source of Ag for the growth of these AgNWs. Furthermore, EDS analysis on older NaCl made the chitosan thin film exhibit even greater conversion of AgCl to AgNWs: with the mean average value percentage of Cl being 0.24% and that of Ag being 56.63%. Fig. S4 (ESI†) shows the raw data of the above discussed EDS data. This analysis suggests that Cl⁻ ions are a key factor for the formation of AgNWs in the solid-state polymer film.

In the second part of this section we investigate the role of cubic AgCl nanoparticles serving as nucleation points for the solid-state growth of AgNWs. In polyol synthesis of AgNWs, cuboidal AgCl nanoparticles function as supreme nucleation sites for the heterogeneous growth of Ag NWs.⁴² In this system, the AgNW growth depends on the secondary addition of silver precursor AgNO₃. In the chitosan thin film synthesis, AgCl nanocubes also appear to form the base for the growth of AgNWs occurring directly from the corners of the cube structures (Fig. 4). The average diameter of the wire growing from these cubic structures is around 80 nm. The SEM images of Fig. 4 are the first depiction of this kind of AgCl based AgNW growth in the solid state. The experiments of excluding addition of NaCl in the synthesis process showed no

formation of AgCl nanocubes on the surface of the chitosan film (Fig. S2, ESI†) and, as a result, no growth of Ag NWs on the same.

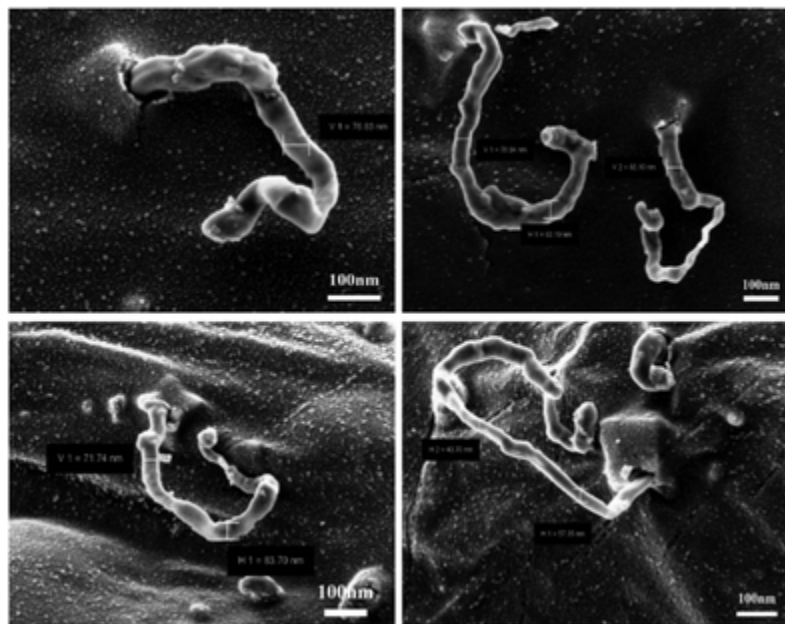


Fig. 4 SEM images of Ag NW growth from the corners of the cubic AgCl nanostructures.

Growth *vs.* time analysis

The AgNWs generated from the chitosan thin film process are irregular and do not possess the same overall morphology or structure that has been generated by other processes.^{18,19,27} During our experiments it became clear that the process of AgNW growth *via* this solid state chitosan film is a continual process that includes both longitudinal growth and lateral growth. The lateral growth means the increasing diameter of the AgNW with time. To determine the rate of growth and the manner of the Ag NW growth, we examined the growth of these Ag NWs over time using SEM. Varying time as a synthesis factor for AgNW growth has been reported in solution processing.⁴³ In this report, the aging of silver crystal seeds in synthesis solution yields more twinned crystal seeds, which act as nucleation bases for further growth of uniform silver nanowires. Similarly, to examine the growth process of Ag NWs on a solid-state chitosan thin film, we measured the diameter and length of the solid state grown AgNWs over the course of seven weeks from week 0 to week 7. In this study, the Ag/chitosan thin films with a 5 nm Au/Pd thin coating were prepared using a chitosan solution that contains 100 mM NaCl and 50 mM AgNO₃.

At week 0 from immediate SEM, we observed that the surface of the chitosan thin film was covered with AgCl cubic nanoparticles (Fig. S8, ESI†). Then metallic Ag protrusions extend from the corners of the AgCl cubes at week 1. By the end of week one, nascent AgNWs can be clearly observed from the corners of the AgCl cubes (Fig. S9, ESI†). At week 2 we observed a marked increase in the number of AgNWs on the film (Fig. S10, ESI†). The week 2 old Ag NWs also exhibited a higher aspect ratio with an increase in the diameter of $\sim 135 \pm 15$ nm (Fig. S10 and Table S1, ESI†). By week 4, we observed a significant increase in both the number of

AgNWs and the length of these nanowires (Fig. S11, ESI†). The AgNWs have a significantly larger diameter of $\sim 400 \pm 50$ nm and a length of $\sim 28 \pm 2$ μm (Fig. S12 and Table S1, ESI†). Fig. 5 shows a graphical plot of the dependence of the AgNW length and width with respect to the age of the film in weeks.

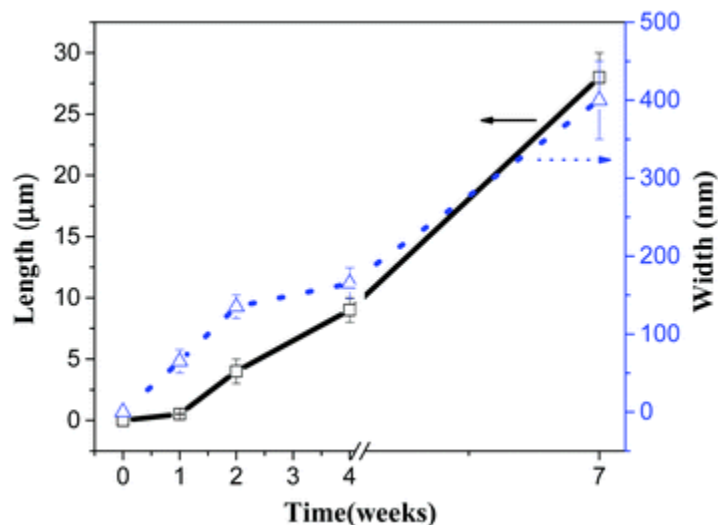


Fig. 5 Length and width of the Ag NWs varying with aging of the film in weeks with represented error bars. The aspect ratio of length to diameter is shown in Fig. S13 and S14 (ESI†).

Discussion

We present the key factors and conditions for unique solid state AgNW growth. Three key conditions/factors have been investigated thoroughly. (1) The role of oxidative etching in AgNW growth at the solid state level is studied by over exposing the Ag-based composite film to oxygen or by covering the film with a thin metal coating or with a self-assembled polymer bead layer. This study is strongly supported by presented SEM images of the AgNW growth over time. It suggests that oxygen deficiency is necessary for the Ag^+ ion reduction and following Ag crystallization and growth. (2) The role of NaCl is investigated on a par with a similar kind of investigation performed in a solution synthesis process.⁴² Our results suggest that a mixture of NaCl and AgNO_3 converts to AgCl nanocubes and at the same time forming Ag NPs in the reaction process. The AgCl nanocubes further form nucleation spots for the growth of AgNWs with a reduction process assisted by chitosan. The EDS experiments show the consumption of AgCl slowly with an increase in the growth of AgNW length with time. (3) Continual growth of Ag NWs with respect to aging of the film is studied and presented with detailed analysis with the help of SEM images. The ability of AgNWs to grow outward from the polymer film up to a length of 28 μm shows the continuous supply of Ag^+ ions from within the film, like nutrients for a sprouted seed. This solid-state, bottom-up, AgCl nucleated and continual growth process of AgNWs is schematically depicted in Scheme 2. The AgNW growth pathway resembles quite closely the natural process of growth of sprouts and the science behind its growth process from a seed. This process is a continual growth process, where the seed takes its “nutrient” source from the film and keeps growing outward.

Conclusions

In this paper we describe factors that control the growth of AgNWs in a chitosan solid state medium. The solution used for the growth film is prepared by mixing AgNO₃ in dissolved chitosan solution with addition of NaCl. The AgCl nanocubes formed on the film become the spots for the growth of AgNWs. The influence of Cl⁻ ions and AgCl NPs on the growth of Ag NWs is examined, and Cl⁻ is needed for the formation of AgCl. The edges of the AgCl nanocubes are the nucleation sites for the AgNWs. We show that like the solution-based AgNW synthetic process where oxidative etching has a significant inhibitory role, the reported AgNW growth presents a new way of blocking the oxidative etching effect on the growth by coating a metal film at the top of the Ag/chitosan matrix film. XRD analysis shows the dominant $\langle 111 \rangle$ phase of the Ag crystal structure of the AgNWs. The formation of AgNWs is a unique self-growth process involving Ag⁺ reduction in the polymer film and depicted as a proposed mechanism like “seed sprouting” at ambient conditions with oxygen deficiency. The Ag⁺ in the film is the “nutrient” source for the AgNW growth with respect to the aging of the substrate film. With all the findings, this article lays a foundation for a new avenue to bottom-up synthesis of AgNWs. A better control of the growth in a patterned platform is underway.

Experimental

Materials

Chitosan (MW: molecular weight: 150 000, 1.5% w/v), AgNO₃ (>99%), acetic acid (70% diluted solution) and NaCl of ultra-pure grade were bought from Sigma-Aldrich.

Film preparation

A synthetic scheme of the AgNWs in the solid state and the choice of specific concentrations of silver precursor AgNO₃ for high yield in growth are reported elsewhere.¹³ In brief, we dissolved chitosan flakes in 10 ml of water with addition of 1% acetic acid (500 μL) (V/V) solution and 100 mM concentration of NaCl (with various volumes in mL). This chitosan solution was mixed using a magnetic stirrer for 24 h until all the chitosan flakes were dissolved, and a viscous solution was formed. 5 ml of 50 mM solution of AgNO₃ was added to the above chitosan solution. A white precipitate was formed during the mixing process and indicated the reduction of the Ag ion. The chitosan/reduced silver solution was sonicated for several hours until the formation of plasmonic colors, *i.e.*, the white precipitate turned yellow and then to pinkish brown when the reaction was stopped and the sample was stored until further characterization.¹⁴ The obtained chitosan/Ag solution is made into films by drop casting 400 μL of the solution on polyethylene terephthalate (PET) substrates and dried at 50 °C until the chitosan/Ag film peels itself from the PET. This volume of the film was chosen based on the number of trials of forming films with different volumes of the solution and the growth of AgNWs on the films was verified using SEM.

Characterization

The morphology including the shape and size of the nanoparticles was characterized using a Zeiss Auriga FIB/SEM scanning electron microscope. Polymer film samples were coated with a

5 nm-thick layer of gold–palladium (Au/Pd) using a Leica EM ACE200. Scale bars were added using ImageJ software. Elemental analysis was performed by energy-dispersive X-ray spectroscopy analysis using a Hitachi S-4800-I FESEM w/Backscattered Detector & EDX to verify the presence of AgNPs and/or AgNWs. The optical properties of the Ag film and solution were evaluated by ultraviolet-visible spectroscopy (UV-Vis spectroscopy, Varian Cary 6000i), and XRD (Aligent) was used for structural analysis of the Ag film.

Conflicts of interest

There are no conflicts to declare.

Acknowledgements

This work was partially supported by an US NIH grant (1R15EB024921-01), and North Carolina State fund through the Joint School of Nanoscience and Nanoengineering (JSNN). This work was performed at the JSNN, a member of South Eastern Nanotechnology Infrastructure Corridor (SENIC) and the National Nanotechnology Coordinated Infrastructure (NNCI), which is supported by the National Science Foundation (ECCS-1542174).

Footnote

† Electronic supplementary information (ESI) available. See <https://doi.org/10.1039/C8NJ05729J>.

Notes and references

1. N. O. Weiss and X. Duan , *Proc. Natl. Acad. Sci. U. S. A.*, 2013, **110** , 15171 —15172 .
2. R. G. Hobbs , N. Petkov and J. D. Holmes , *Chem. Mater.*, 2012, **24** , 1975 —1991 .
3. M. Koto *J. Cryst. Growth*, 2014, **391** , 72 —77 .
4. H. K. Yu and J.-L. Lee , *Sci. Rep.*, 2014, **4** , 6589 .
5. P. Zhang , I. Wyman , J. Hu , S. Lin , Z. Zhong , Y. Tu , Z. Huang and Y. Wei , *Mater. Sci. Eng., B*, 2017, **223** , 1 —23 .
6. S. E. H. Murph , C. J. Murphy , A. Leach and K. Gall , *Cryst. Growth Des.*, 2015, **15** , 1968 —1974 .
7. Y. Xia , P. Yang , Y. Sun , Y. Wu , B. Mayers , B. Gates , Y. Yin , F. Kim and H. Yan , *Adv. Mater.*, 2003, **15** , 353 —389 .
8. J. Yao , Y. Wang , K.-T. Tsai , Z. Liu , X. Yin , G. Bartal , A. M. Stacy , Y.-L. Wang and X. Zhang , *Philos. Trans. R. Soc., A*, 2011, **369** , 3434 —3446 .
9. J. Joo , B. Y. Chow , M. Prakash , E. S. Boyden and J. M. Jacobson , *Nat. Mater.*, 2011, **10** , 596 .
10. H.-W. Jang , B.-Y. Hwang , K.-W. Lee , Y.-M. Kim and J.-Y. Kim , *AIP Adv.*, 2018, **8** , 025303 .
11. Z. Tang and N. A. Kotov , *Adv. Mater.*, 2005, **17** , 951 —962 .
12. M. Heiss , Y. Fontana , A. Gustafsson , G. Wüst , C. Magen , D. D. O’Regan , J. W. Luo , B. Ketterer , S. Conesa-Boj , A. V. Kuhlmann , J. Houel , E. Russo-Averchi , J. R. Morante , M. Cantoni , N. Marzari , J. Arbiol , A. Zunger , R. J. Warburton and A. Fontcuberta i Morral , *Nat. Mater.*, 2013, **12** , 439 .
13. R. Chandran , H. Chevva , Z. Zeng , Y. Liu , W. Zhang , J. Wei and D. LaJeunesse , *Mater. Today*, 2018, **1** , 22 —28 .

14. H.Chevva, R.Chandran, D.LaJeunesse and J.Wei, 2017 IEEE 17th International Conference on Nanotechnology (IEEE-NANO), 2017, 885889, 10.1109/NANO.2017.8117319.
15. N. F. Za'bah , K. S. K. Kwa , L. Bowen , B. Mendis and A. O'Neill , *J. Appl. Phys.*, 2012, **112** , 024309 .
16. S. F. A.Rahman, N. A.Yusof, M. N.Hamidon, R. M.Zawawi and U.Hashim, 2014 IEEE International Conference on Semiconductor Electronics (ICSE2014), 2014, pp. 64–67.
17. G. Pennelli *Microelectron. Eng.*, 2009, **86** , 2139 —2143 .
18. G.-C. He , M.-L. Zheng , X.-Z. Dong , F. Jin , J. Liu , X.-M. Duan and Z.-S. Zhao , *Sci. Rep.*, 2017, **7** , 41757 .
19. H. Oh , J. Lee , J.-H. Kim , J.-W. Park and M. Lee , *J. Phys. Chem. C*, 2016, **120** , 20471 —20477 .
20. J. Huang , D. Fan , Y. Ekinici and C. Padeste , *Microelectron. Eng.*, 2015, **141** , 32 —36 .
21. A. Wolfsteller , N. Geyer , T. K. Nguyen-Duc , P. Das Kanungo , N. D. Zakharov , M. Reiche , W. Erfurth , H. Blumtritt , S. Kalem , P. Werner and U. Gösele , *Thin Solid Films*, 2010, **518** , 2555 —2561 .
22. T. L. Yang , C. T. Pan , Y. C. Chen , L. W. Lin , I. C. Wu , K. H. Hung , Y. R. Lin , H. L. Huang , C. F. Liu , S. W. Mao and S. W. Kuo , *Opt. Mater.*, 2015, **39** , 118 —124 .
23. D. Li , T. Han , L. Zhang , H. Zhang and H. Chen , *R. Soc. Open Sci.*, 2017, **4** , 170756 .
24. R. Gottesman , A. Tangy , I. Oussadon and D. Zitoun , *New J. Chem.*, 2012, **36** , 2456 —2459 .
25. L. Liu , C. He , J. Li , J. Guo , D. Yang and J. Wei , *New J. Chem.*, 2013, **37** , 2179 —2185 .
26. D. Zhang , L. Qi , J. Yang , J. Ma , H. Cheng and L. Huang , *Chem. Mater.*, 2004, **16** , 872 —876 .
27. X.-F. Pan , H.-L. Gao , Y. Su , Y.-D. Wu , X.-Y. Wang , J.-Z. Xue , T. He , Y. Lu , J.-W. Liu and S.-H. Yu , *Nano Res.*, 2018, **11** , 410 —419 .
28. R. Kalaivani , M. Maruthupandy , T. Muneeswaran , A. Hameedha Beevi , M. Anand , C. M. Ramakritinan and A. K. Kumaraguru , *Frontiers in Laboratory Medicine*, 2018, **2** , 30 —35 .
29. M. Bilal , T. Rasheed , H. M. N. Iqbal , C. Li , H. Hu and X. Zhang , *Int. J. Biol. Macromol.*, 2017, **105** , 393 —400 .
30. X. Huang , X. Bao , Z. Wang and Q. Hu , *RSC Adv.*, 2017, **7** , 34655 —34663 .
31. M. Flores-González , M. Talavera-Rojas , E. Soriano-Vargas and V. Rodríguez-González , *New J. Chem.*, 2018, **42** , 2133 —2139 .
32. R. Long , S. Zhou , B. J. Wiley and Y. Xiong , *Chem. Soc. Rev.*, 2014, **43** , 6288 —6310 .
33. A. Amirjani , D. H. Fatmehsari and P. Marashi , *J. Exp. Nanosci.*, 2015, **10** , 1387 —1400 .
34. M. R. Johan , N. A. K. Aznan , S. T. Yee , I. H. Ho , S. W. Ooi , N. Darman Singho and F. Aplop , *J. Nanomater.*, 2014, **2014** , 7 .
35. Z. Li , J. S. Okasinski , J. D. Almer , Y. Ren , X. Zuo and Y. Sun , *Nanoscale*, 2014, **6** , 365 —370 .
36. S. Coskun , B. Aksoy and H. E. Unalan , *Cryst. Growth Des.*, 2011, **11** , 4963 —4969 .
37. Y. Xia , Y. Xiong , B. Lim and S. E. Skrabalak , *Angew. Chem., Int. Ed.*, 2009, **48** , 60 —103 .
38. R. Chandran , K. Nowlin and R. D. LaJeunesse , *Polymers*, 2018, **10** , 218 .
39. M. H. Kahsay , D. RamaDevi , Y. P. Kumar , B. S. Mohan , A. Tadesse , G. Battu and K. Basavaiah , *OpenNano*, 2018, **3** , 28 —37 .
40. C. Han , L. Ge , C. Chen , Y. Li , Z. Zhao , X. Xiao , Z. Li and J. Zhang , *J. Mater. Chem. A*, 2014, **2** , 12594 —12600 .

41. J. Song , J. Roh , I. Lee and J. Jang , *Dalton Trans.*, 2013, **42** , 13897 —13904 .
42. W. M. Schuette and W. E. Buhro , *ACS Nano*, 2013, **7** , 3844 —3853 .
43. S. Chang , K. Chen , Q. Hua , Y. Ma and W. Huang , *J. Phys. Chem. C*, 2011, **115** , 7979 —7986 .